

# Optical characterization of *Pseudomonas fluorescens* on meat surfaces using time-resolved fluorescence

Alain Bouchard\*

Julie Fréchette

Marcia Vernon

Jean-François Cormier

René Beaulieu

Institut National d'Optique  
Parc Technologique du Québec Métropolitain  
2740, rue Einstein  
Sainte-Foy, Québec, G1P 4S4 Canada  
E-mail: Rene.Beaulieu@ino.ca

Réal Vallée

Université Laval  
Center for Optics Photonics and Lasers  
Faculté des Sciences et de Génie  
Pavillon Alexandre-Vachon  
Québec, G1K 7P4 Canada

Akier Assanta Mafu

Agriculture and Agri-Food Canada  
Food Research and Development Centre  
3600 Casavant Boulevard West  
Saint Hyacinthe, Québec, J2S 8E3 Canada

**Abstract.** A scanning optical system for the detection of bacteria on meat surfaces based on fluorescence lifetime and intensity measurements is described. The system detects autofluorescent light emitted by naturally occurring fluorophores in bacteria. The technique only requires minimal sample preparation and handling, thus the chemical properties of the specimen are preserved. This work presents the preliminary results obtained from a time-resolved fluorescence imaging system for the characterization of a nonpathogenic gram-negative bacteria, *Pseudomonas fluorescens*. Initial results indicate that the combination of fluorescence lifetime and intensity measurements provides a means for characterizing biological media and for detecting microorganisms on surfaces. © 2006 Society of Photo-Optical Instrumentation Engineers. [DOI: 10.1117/1.2162166]

**Keywords:** fluorescence lifetime; bacteria; real time; noncontact; agrifood; *Pseudomonas fluorescens*; meat.

Paper 05014RR received Jan. 19, 2005; revised manuscript received Aug. 10, 2005; accepted for publication Aug. 29, 2005; published online Jan. 24, 2006. This paper is a revision of a paper presented at the SPIE conference on Biomedical Vibration Spectroscopy and Biohazard Detection Technologies, Jan. 2004, San Jose, California. The paper presented there appears (unrefereed) in SPIE proceedings Vol. 5321.

## 1 Introduction

The Centers for Disease Control and Prevention estimates that 76 million Americans are affected by foodborne illness each year.<sup>1</sup> The most serious cases among these necessitate approximately 325,000 hospitalizations, costing several billions of dollars, and cause about 5000 deaths annually. A great proportion of these cases are caused by known pathogenic microorganisms, such as *Escherichia coli* O157:H7, *Campylobacter*, *Listeria monocytogenes*, salmonella, and *shigella*. Meat, poultry, fish, eggs, dairy products, and in particular undercooked ground meat, are all excellent media for bacterial proliferation.<sup>2</sup> As a consequence, detection of bacterial contamination is of great interest to the meat processing industry.

Current methods of detection for pathogens and spoilage microorganisms are time consuming, the majority of which require culture and incubation periods that necessitate a waiting period of 18 to 72 h for the results to be available. For example, a nucleic acid detection method based on polymerase chain reaction (PCR) is one of the most rapid, with test times on the order of 18 h for salmonella.<sup>3</sup>

As bacteria emit fluorescence after ultraviolet light excitation, optical techniques are now being developed that will allow for their detection. In one study, differentiation between five bacterial species based on fluorescence decay times has been demonstrated under well-controlled conditions.<sup>4</sup> Bacterial fluorescence lifetimes were measured *in vitro* at 430, 487, and 514 nm after selective excitation at 340, 405, and

430 nm on bacterial suspensions containing approximately  $10^8$  organisms/mL. In another study, imaging of six different strains of bacteria on meat surfaces was done using 488-nm continuous-wave laser illumination.<sup>5</sup> Based on this initial work, it appears possible that fluorescent lifetime signatures of bacteria may provide the necessary information to allow for their detection and identification on complex substrates such as meat.

This work presents a real-time method for detecting and identifying bacterial contamination on animal carcasses and on meat. The method is based on the autofluorescence of bacteria and their by-products on meat surfaces after laser excitation of the sample with a pulsed 400-nm laser beam. The system measures fluorescence lifetime and intensity. The opportunity to use a real-time noncontact technique would be of great interest for the food industry, as it requires minimal sample preparation and handling. The following sections describe the methodology and the results of the characterization by time-resolved fluorescent imaging of slices of beef meat inoculated with *Pseudomonas fluorescens*.

## 2 Materials and Methods

### 2.1 System Description

Figure 1 presents a schematic representation of the system. Samples are placed on an *x-y-z* translation stage for scanning, and are illuminated by a pulsed laser beam emitted by a laser diode (PicoQuant GmbH, LDH-P-C-400; driver PicoQuant GmbH, PDL-800-B). The 400-nm beam irradiates the sample with a power of 1.2 mW, has a repetition rate of 40 MHz,

\*Current affiliation: STS.

Address all correspondence to René Beaulieu, Biophotonic, INO, 2740, Einstein Street, Sainte-Foy, Québec, G1P 4S4 Canada. Tel: 418-657-7006. Fax: 418-657-7009. E-mail: Rene.Beaulieu@ino.ca

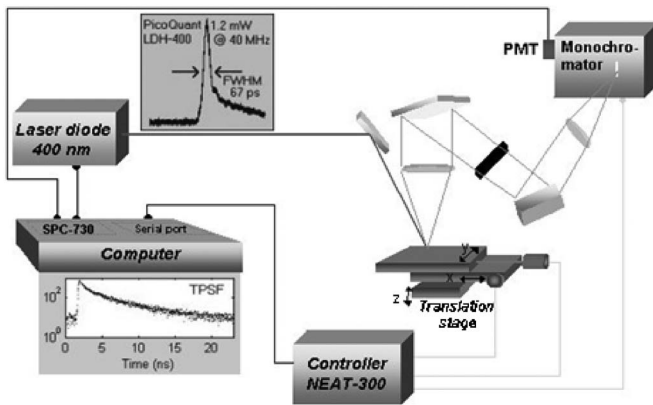


Fig. 1 Schematic of the experimental setup for time-resolved measurement.

and has pulse width of 67 ps [full width at half maximum (FWHM)]. The beam strikes the sample at an incident angle of 13 deg and illuminates a  $1 \times 2\text{-mm}^2$  area. In the reported experiments, the scanning is done with a step of 0.5 mm with a number of points of  $20 \times 21$  (total of 420 points) over the  $1\text{-cm}^2$  surface.

Fluorescent emissions from the sample are directed into a monochromator (Bentham M300E), and a photomultiplier tube (Becker & Hickl GmbH, PMH-100-3) detects the light. The detector is connected to a constant fraction discriminator input of a time-correlated single photon counting (TCSPC) board (Becker & Hickl GmbH, SPC-730). This TCSPC module collects time-resolved fluorescence decay data in the form of a temporal point spread function (TPSF) for each of the scan points, with a time span of 25 ns and 1024 points, thus giving an effective time resolution of 24.4 ps.

## 2.2 Bacterial Culture Preparation

A strain of the spoilage bacteria *Pseudomonas fluorescens* obtained from the Food Research and Development Center, Agriculture and Agri-Food Canada (Saint Hyacinthe, Québec), was used for the experiments. *P. fluorescens* is a gram-negative obligate aerobic bacillus, motile by one or several polar flagella. *P. fluorescens* is a psychrotroph and is often responsible for the spoilage of refrigerated meat, fish, eggs, and dairy products. It produces a water soluble, fluorescent pigment called pyoverdine, also known as fluorescein.<sup>6</sup> Pyoverdine is responsible for scavenging free iron in the medium and for its transport through the outer membrane of bacteria. Production of pyoverdine by bacteria is regulated by iron availability in the cell's environment, with more pigment produced in iron-deficient conditions.<sup>7</sup>

Cultures were grown on Trypticase Soy Agar (TSA, Becton-Dickinson BBL prepared culture media 221236) plates and in Trypticase Soy Broth (TSB, Becton-Dickinson BBL 297354) tubes. Culture was grown to a concentration of approximately  $2 \times 10^8$  UFC/mL by the incubation of the tubes for 24 h at 30°C. Afterward, this broth was sequentially diluted (1/10) six times in saline water (Becton-Dickinson BBL 221818, 8.5 g NaCl per liter of water). Inoculation culture plates were prepared by spreading 200  $\mu\text{L}$  of the result-

ing  $10^{-6}$  dilutions on an agar plate. These culture plates were incubated for 24 h at 30°C to give 20 to 40 isolated colonies of *P. fluorescens* of about 1 mm in diameter. Following incubation, the cultures were refrigerated (4°C) for use within one to six hours.

## 2.3 Meat Sample Preparation

Commercially available, 6-mm-thick frozen slices of beef (eye of round) were used in the experiments. Slices were thawed to 4°C 12 to 24 h before scans. Samples of  $25 \times 25 \text{ mm}^2$  were cut from the slices and placed on a clean microscope slide prior to scanning. The uncovered sample was placed in the scanning system, and a Peltier effect cell placed under the slide regulated the sample temperature. Inoculation of the meat sample was made by direct contact with the prepared cultures for 30 s. Standard microbiological techniques have measured an initial contamination of less than 3 UFC/cm<sup>2</sup> on the meat prior to inoculation.

## 2.4 Experiments

An initial background fluorescence image of the meat specimens was recorded prior to inoculation. A  $1\text{-cm}^2$  area in the center of the specimen was scanned. The initial scan helps to determine the fluorescence background properties of the meat that is afterward compared to the fluorescent emissions of the inoculated sample. Such comparisons serve to establish the extent of contamination of the sample. Specimen temperature was stabilized by the Peltier effect cell, depending on the measurement series. Fluorescence decay data (TPSFs) were saved at a resolution of 24.4 ps per time bin.

## 3 Results

Monoexponential and biexponential fluorescence decay models were fitted to each TPSF. Equation (1) describes the monoexponential decay model:

$$I(t) = I_0 \cdot \exp(-t/\tau), \quad (1)$$

where  $I_0$  is the relative intensity,  $t$  is the time, and  $\tau$  is the fluorescence lifetime, both expressed in nanoseconds. The biexponential decay model is written as:

$$I(t) = F_1 \cdot \exp(-t/\tau_1) + F_2 \cdot \exp(-t/\tau_2), \quad (2)$$

where  $F_1$  and  $F_2$  are the relative intensities associated with two lifetimes,  $\tau_1$  and  $\tau_2$ , respectively.

Monoexponential models are normally used to fit fluorescence decay data when only one main fluorophore is present in the sample. Biexponential fits may be more appropriate for samples containing more than one fluorescent species. Fitting was done using a least-squares algorithm using a reconvolution approach. In this method, convolution of Eqs. (1) or (2) with the instrumental response function (IRF)<sup>8</sup> is done prior to evaluating the goodness of fit with a weighted  $\chi^2$  (chi-squared) parameter. Typical TPSFs and their best-fit decays for *Pseudomonas fluorescens* on meat are shown in Fig. 2. As shown in the lower left and right graphs of Fig. 2, the biexponential decay model represents the data better than a single decay, as evidenced by the even distribution of the residuals about zero. Weighted  $\chi^2$  parameter values of 1.1 and 2.4 have been obtained with the biexponential decay model and the

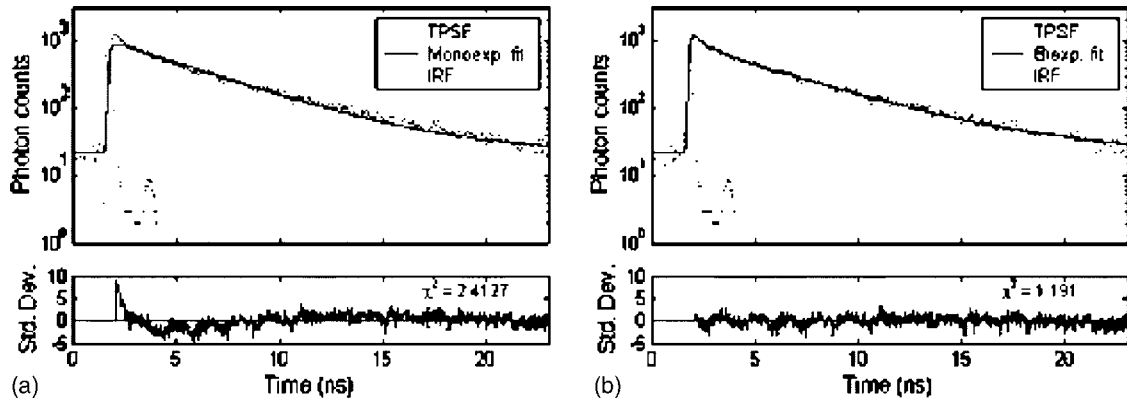


Fig. 2 Typical TPSF and best-fit (a) mono-exponential and (b) bi-exponential decay models from one contaminated sample region.

single decay model, respectively. Based on this information, the analysis has focused on biexponential decay fits.

Figures 3 and 4 present plots of the different parameters of the biexponential decay fit for a 1-cm<sup>2</sup> scan on a noncontaminated area. The fluorescence data were recorded at the peak emission wavelength of fluorescein, 515 nm. The fluorescein is an element of the pyoverdin group. The temperature of the samples was stabilized at 20 °C by a Peltier effect cell. TPSF data were processed at each of the 420 points scanned. These plots show the evolution of the different parameters over a period of 15 h. Using the numerical values, one can find that the variation of  $\tau_1$ ,  $\tau_2$ ,  $F_1$ , and  $F_2$  is approximately 1.2, 3.8, 18, and 13%, respectively. These variations may be due to the dehydration of the meat that produces a bigger concentration of fluorophores. Figure 4 shows that the mean lifetimes and standard deviation of the biexponential decay fit are  $\sim(3.1 \pm 0.3)$  ns and  $\sim(0.5 \pm 0.1)$  ns for  $\tau_1$  and  $\tau_2$ , respectively.

Typical plots for comparing the parameters of the biexponential fits, after initial time, 30 and 150 min after inoculation time are shown in Figs. 5 and 6. After 150 min, the total number of photons collected by the system decreased for inoculated regions. However, the inoculated areas are still visible. Figure 6 shows that the mean lifetimes of the biexponential decay fit for lifetime  $\tau_1$  are significantly different between contaminated and noncontaminated regions 30 min after inoculation (a mean of 4.2 ns versus a mean of 3.2 ns, respectively).

In Figs. 7 and 8, the fluorescence map characteristics of a meat sample containing a large marbled area is shown. The fluorescence intensity of the marbled area is much stronger than the muscle area, and the longer lifetime is statistically well centered around 4.7 ns, as shown in Fig. 8, providing a means to identify the presence of fat and connective tissues in a sample.

Figures 9 and 10 show the decay parameters of the biexponential fit for contaminated and noncontaminated areas at the peak emission wavelength of fluorescein, 515 nm. The temperature of samples 1(S1), 2(S2), 3(S3), and 4(S4) was stabilized at 20, 20, 4, and 37 °C, respectively by a Peltier effect cell. The abscissa represents the following experimental conditions: noncontaminated area at initial time, NC; contaminated area 30 min after inoculation time, C30; noncon-

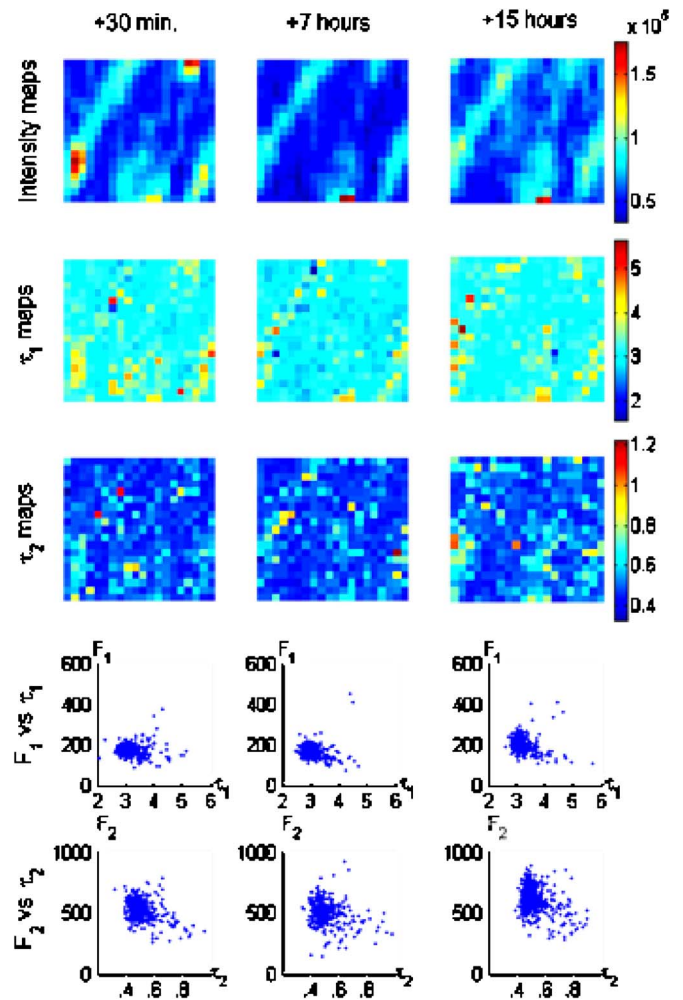
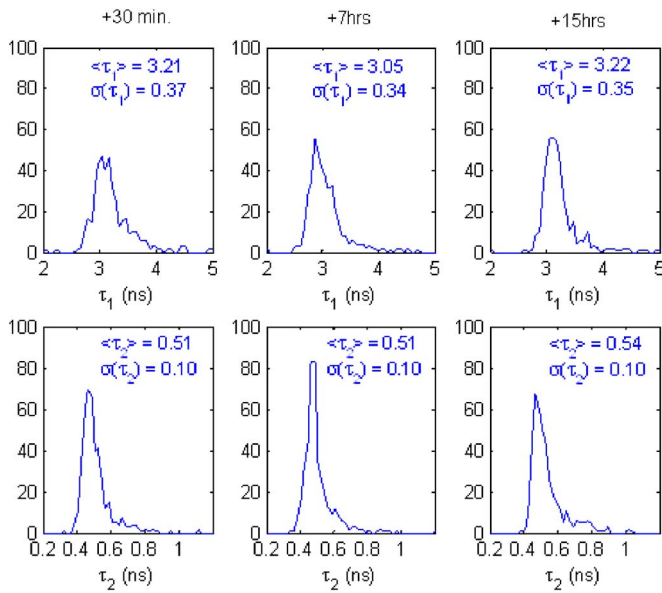
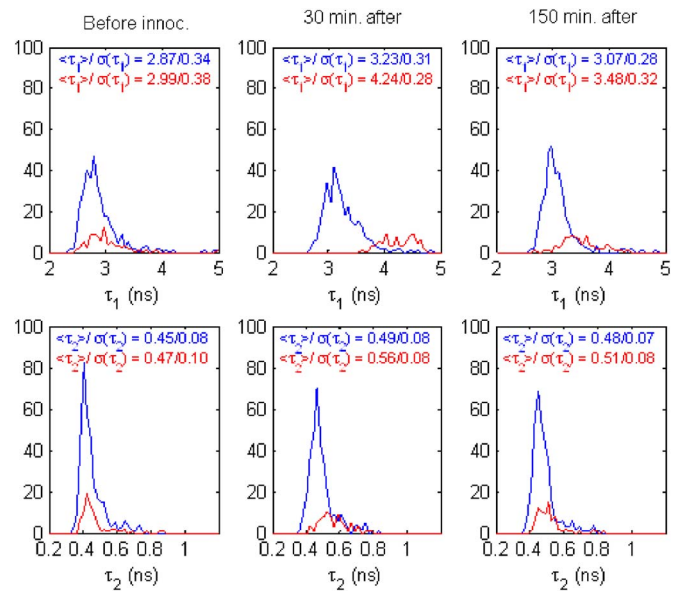


Fig. 3 Plots of the different parameters of the biexponential decay fit for a 1-cm<sup>2</sup> scan on a noncontaminated area. The fluorescence data were recorded at the peak emission wavelength of fluorescein, 515 nm. The temperature of the samples was stabilized at 21 °C by a Peltier effect cell. TPSF data were processed at each of the 420 points scanned. The rows correspond to data taken after 30 min, 7, and 15 h, respectively. The top line shows the integrated intensity plot, the second and third lines show the lifetime maps for  $\tau_1$  and  $\tau_2$ , respectively, while the fourth and fifth lines show a phase plot of the relative intensities in terms of the lifetimes of the biexponential decay model.



**Fig. 4** Histograms showing the statistical distributions of the lifetime data  $\tau_1$  and  $\tau_2$  associated with the scan of a noncontaminated area of Fig. 3.



**Fig. 6** Histograms showing the statistical distributions of the lifetime data  $\tau_1$  and  $\tau_2$  associated with the scan of meat slice inoculated by *P. fluorescens* of Fig. 4(a). The two curves of each plot represent the statistics of the “inoculated” (red) and “noninoculated” (blue) regions.

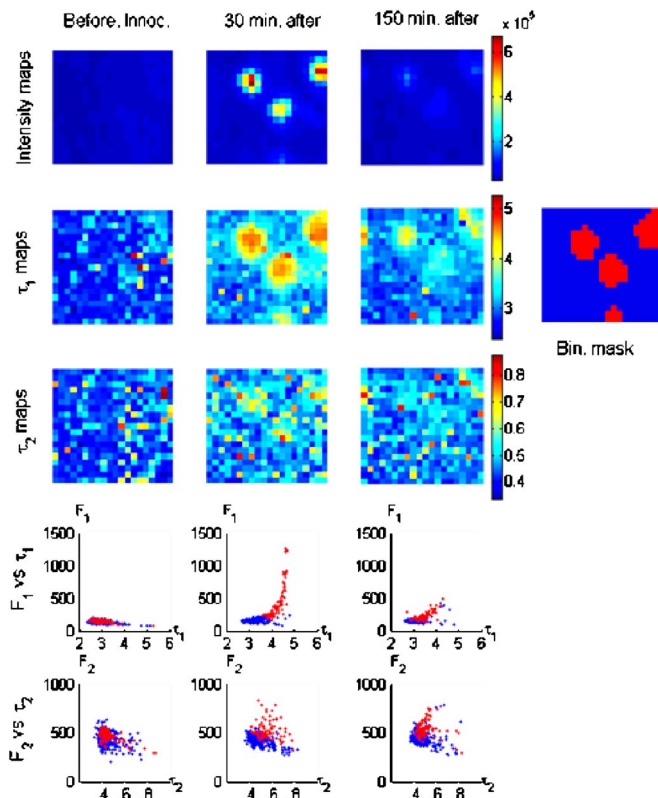


**Fig. 5** Plots of the biexponential decay model parameters for fluorescence data recorded at 515 nm over a 1-cm<sup>2</sup> area on a slice of meat inoculated by *P. fluorescens*. The rows correspond to data taken before, after 30 min, and after 150 min, of inoculation, respectively. The top line shows the integrated intensity plot; the second and third lines show the lifetime maps for  $\tau_1$  and  $\tau_2$ , respectively, while the fourth and fifth lines show a phase plot of the relative intensities in terms of the lifetimes of the biexponential decay model, for the data in the inoculated (red) and noninoculated (blue) regions. Also shown at the right, the binary mask used to separate the regions into inoculated (red) and noninoculated (blue).

taminated area 30 min after inoculation time, NC30; contaminated area 150 min after inoculation time, C150; and noncontaminated area 150 min after inoculation time, NC150. It is important to note that the areas are classified as contaminated or noncontaminated at inoculation time.

As shown in Fig. 9, one can observe that the values of  $F_1$  (continuous lines) are greater for the contaminated area as compared with values of  $F_1$  for the noncontaminated area. Also, the corresponding values for the noncontaminated area do not vary much from initial time up to 150 min.

When observing the data shown in these figures, one can see identical trends in the increase of  $\tau_1$  (dashed lines),  $F_2$  (continuous lines), and  $\tau_2$  (dashed lines) for the contaminated area. Concerning the data that have been obtained with the noncontaminated area, our results indicate that the levels of these parameters are comparable.

## 4 Discussion

Meat is a complex medium and contains a variety of intrinsic fluorophores. The presence of bacteria on the meat modifies the relative quantity of fluorophores and adds new ones either from the organic constituents from the microorganism or its by-products. This modifies the fluorescence emission properties of the specimen, both spectrally and temporally. The intrinsic fluorophores contained in meat and/or *P. fluorescens* colonies that are excitable at 400 nm include nicotinamide adenine dinucleotide (NADH), flavins, pyoverdine, collagen, elastin, lipids, and porphyrins.<sup>9</sup>

Looking back at Figs. 3–8, one may argue that the parameters  $F_1$ ,  $F_2$ ,  $\tau_1$ , and  $\tau_2$  of the biexponential fit show large variability over the 1-cm<sup>2</sup> surface scanned, even for a noncontaminated meat.

Although the variability of parameters  $F_1$  and  $F_2$  can be easily understood from the fact that the medium surface char-

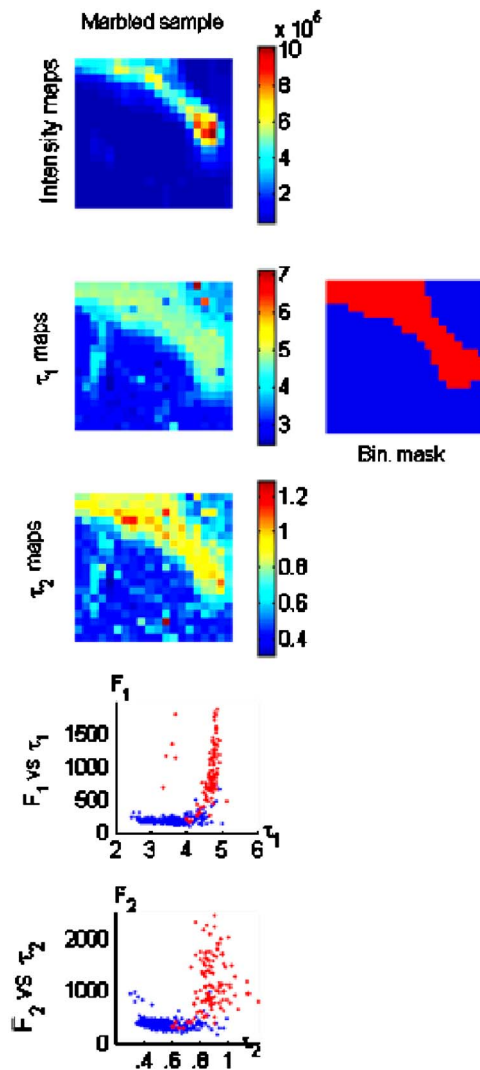


**Fig. 7** Plots of the biexponential decay model parameters for fluorescence data recorded at 515 nm over a 1-cm<sup>2</sup> area on a slice of meat comprising a large marbled area. The top line shows the integrated intensity plot, the second and third lines show the lifetime maps for  $\tau_1$  and  $\tau_2$ , respectively, while the fourth and fifth lines show a phase plot of the relative intensities in terms of the lifetimes of the biexponential decay model, for the data in the marbled (red) and muscle and non-inoculated (blue) regions. Also shown at the right, the binary mask used to separate the regions into “marbled” (red) and “muscle” (blue).

acteristics are varying spatially (more or less fat, muscle, etc...), the values of lifetimes  $\tau_1$  and  $\tau_2$  should be relatively constant if we were in the presence of a medium containing two fluorescent components, placed in a stable chemical environment. Thus, we can conclude that the representation of a complex medium such as meat by a biexponential decay presents some limitations, and that the variability of the fitted parameters can be explained by one or both of the following reasons: 1. more than two fluorescent species are present on the meat surface, and 2. the local variability of pH or other quenchers modify the observed fluorescent lifetimes. In fact, from measurements made on sample areas of muscle, fat, and contaminated regions as pure as possible, we found that the decay lifetimes  $\tau_1/\tau_2$  were centered on 3.1/0.5 ns in the

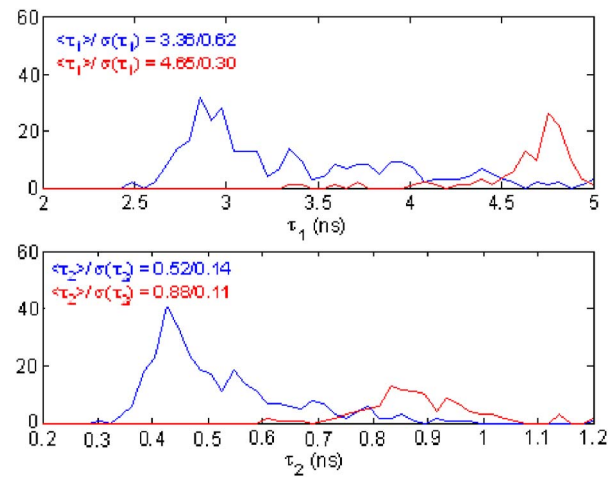


**Fig. 8** Histograms showing the statistical distributions of the lifetime data  $\tau_1$  and  $\tau_2$  associated with the scan of a slice of meat comprising a large marbled area of Fig. 5(a). The two curves of each plot represent the statistics of the “marbled” (red) and “muscle” (blue) regions.

muscle, 4.7/1.0 ns in the fat and connective tissues, and 4.2/0.5 ns on contaminated areas. Thus, lifetimes extracted from a biexponential fit of the decay curve could be used to discriminate between these three types of regions on meat, even with the large variability observed.

One final point to mention regarding the variability of the measured lifetimes and intensities is the fact that the limited spatial resolution of the measurements (1-mm<sup>2</sup> spot) defines regions of analysis that comprise many compounds. The situation would probably be different if we were using a microscopic configuration where fat, muscle, and contaminated regions could be spatially isolated from one another. Moreover, the analysis of the different regions on a single sample required the creation of a spatial mask, based on the intensity level, to select the regions from which to build the statistics for  $F_1$ ,  $F_2$ ,  $\tau_1$ , and  $\tau_2$ . The results could probably be improved by rejecting the regions on the edge of the mask, since they are prone to contain a mix of compounds and thus increase the variance of the statistics, due to the fact that a biexponential decay fit on a mixture of more than two components necessarily increases the variance of the statistics of the fitted parameters. Finally, it is also worth noting that using a multi-exponential fit with more than two exponentials is possible, but in practice is very unstable and requires large dynamic range in the measurement to reveal the presence of the lowest intensity component.

The first decay component of the biexponential fit for the contaminated specimens appears to be associated with fluorescein produced by the bacteria, and with flavins, other major fluorophores of tissues and cells. The fluorescence lifetime of pyoverdine (fluorescein) is reported to be 4 to 6 ns,<sup>7</sup> and the long lifetime component of flavin adenine dinucleotide (FAD) is reported to be 3.38 ns.<sup>8</sup> Our results show that the intensity component  $F_1$  associated with bacterial fluorescein is high just after the inoculation, then decreases rapidly over 2.5 h. Since meat contains high levels of iron (relative to the agar growth medium), it makes sense that fluorescein production rates showed a drop during the adaptation period. As men-

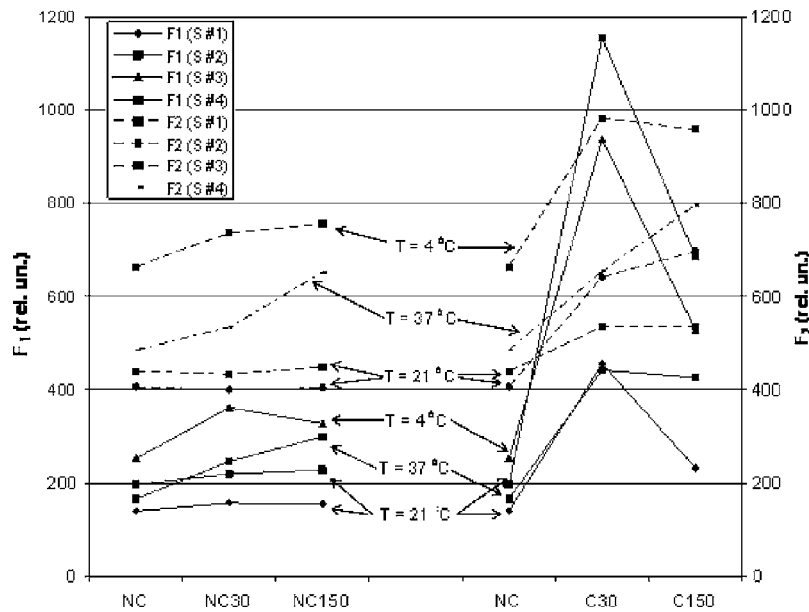


**Fig. 9** Relative intensities  $F_1$  (continuous lines) and  $F_2$  (dashed lines) for contaminated area and noncontaminated area at the peak emission wavelength of fluorescein, 515 nm. The temperature of samples 1(S1), 2(S2), 3(S3), and 4(S4) was stabilized at 21, 21, 4, and 37 °C, respectively. The abscissa represents the following experimental conditions: noncontaminated area at initial time, NC; contaminated area 30 min after inoculation time, C30; noncontaminated area 30 min after inoculation time, NC30; contaminated area 150 min after inoculation time, C150; and noncontaminated area 150 min after inoculation time, NC150.

tioned previously, production of fluorescein is regulated by the availability of iron with higher production in iron deficient conditions.<sup>7</sup> Meat dehydration and oxidation, bacterial viability, cellular lysis, and long-term adaptation, which are known to affect sample fluorescence, may be responsible for other variations in the images.

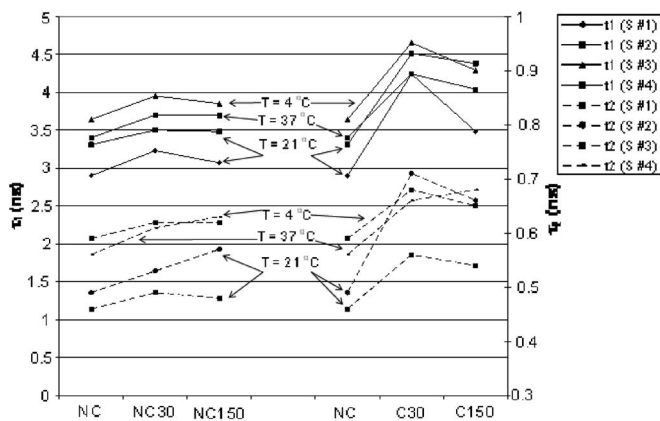


**Fig. 10** Fluorescence lifetimes  $\tau_1$  (continuous lines) and  $\tau_2$  (dashed lines) for contaminated area and noncontaminated area at the peak emission wavelength of fluorescein, 515 nm. The temperature of samples 1(S1), 2(S2), 3(S3), and 4(S4) was stabilized at 21, 21, 4, and 37 °C, respectively. The abscissa represents the following experimental conditions: noncontaminated area at initial time, NC; contaminated area 30 min after inoculation time, C30; noncontaminated area 30 min after inoculation time, NC30; contaminated area 150 min after inoculation time, C150; and noncontaminated area 150 min after inoculation time, NC150.

### 5 Conclusion

A fluorescence lifetime imaging system is constructed as a new tool for the detection and identification of bacterial contamination on surfaces. The apparatus allows noncontact scanning of meat samples, and collects the intrinsic fluorescent emissions following laser excitation at 400 nm. A biexponential decay model is fitted to the fluorescence data recorded by a single photon counting system, and appears to be appropriate for this type of data. Colonies of *Pseudomonas fluorescens*, a spoilage bacterium, are detected and imaged on meat samples. Contaminated regions are clearly indicated. Although this study concentrates on 515-nm fluorescent emissions, other wavelength regions may be collected and imaged with this system. Other excitation wavelengths can also be considered. With additional research on a greater variety of samples and bacterial growth conditions, insight into the development of a practical, real-time fluorescence imaging system for the detection and identification of microorganisms on meat may be made.

### References

- Centers for Disease Control and Prevention, see <http://www.cdc.gov/>
- Agriculture and Agri-Food Canada, see <http://www.agr.gc.ca/>
- D. I. Ellis and R. Goodacre, "Rapid and quantitative detection of the microbial spoilage of muscle foods: current status and future trends," *Trends Food Sci. Technol.* **12**, 414–424 (2001).
- R. A. Dalterio, W. H. Nelson, D. Britt, J. F. Sperry, J. F. Tanguay, and S. L. Suib, "The steady-state and decay characteristics of primary

- fluorescence from live bacteria," *Appl. Spectrosc.* **41**, 234–241 (1987).
5. P. J. Hilton, "Laser induced fluorescence imaging of bacteria," *Proc. SPIE* **3491**, 1174–1178 (1998).
  6. L. M. Prescott, J. P. Harley, and D. A. Klein, *Microbiology*, pp. 503–504, Mc-Graw-Hill, New York (2002).
  7. N. Folschweiller, J. Gallay, M. Vincent, M. A. Abdallah, F. Pattus, and I. J. Schalk, "The interaction between pyoverdinin and its outer membrane receptor in *Pseudomonas aeruginosa* leads to different conformers: A time-resolved fluorescence study," *Biochemistry* **41**, 14951–14601 (2002).
  8. J. R. Lakowicz, "Time-domain lifetime measurements," in *Principles of Fluorescence Spectroscopy*, 2nd ed., pp. 1–184, Kluwer Academic, Plenum Publishers, New York (1999).
  9. N. Ramanujam, "Fluorescence spectroscopy in vivo," in *Encyclopedia of Analytical Chemistry*, R. A. Meyers, Ed., pp. 20–56, John Wiley & Sons Ltd, Chichester, UK (2000).